Magnetization and Electric Properties of Pr-doped ZnO

NAOKI OHASHI[†], SHUN MITARAI[‡] & OSAMU FUKUNAGA[§]

Department of Inorganic Materials, Faculty of Engineering, Tokyo Institute of Technology, 2-12-1 O-okayama, Meguro, Tokyo 152-8552, Japan. E-mail: nohashi@ceram.titech.ac.jp

JUNZO TANAKA

National Institute for Research in Inorganic Materials, 1-1 Namiki, Tsukuba, Ibaraki 305-0044, Japan

Abstract. Magnetic susceptibility of ZnO-varistors doped with Pr-ion was measured to elucidate the valence state of the Pr-ion and the effect of thermal treatment. Magnetic susceptibility $\chi(T)$ of the Pr-ion obeyed Curie-Weiss law, from which its valence state was estimated. The valence state of the Pr-ion varied with annealing condition of specimens, and it was indicated that the Pr-ion in ZnO ceramics was more reducible in comparison with pure PrO_x ceramics. Nonlinear current-voltage characteristics was diminished with the reduction of the valence state of Pr ions. According to Auger electron spectra, the Pr-ions segregated at grain boundaries in ZnO ceramics.

1. Introduction

Nonlinear current-voltage (*I-V*) characteristics appear in ZnO ceramics with doping bismuth oxide [1] or praseodymium oxide [2]. In general, it is known that the nonlinear *I-V* characteristics are due to the interfacial states formed at grain boundaries [3–6].

Chemical composition and electronic state at grain boundaries in ZnO ceramics have been studied by some spectroscopic methods to discuss the formation mechanism of the interfacial states. Tanaka et al. [7–10] have applied an Auger electron spectroscopy method to analyze the chemical composition of grain boundaries in the ZnO ceramics doped with bismuth oxide (Bi-ZnO). They found that the bismuth ions segregated at the grain boundaries and an oxygen content decreased corresponding to the increase of the bismuth content: i.e., the grain boundaries in the Bi-doped ZnO ceramics were reduced by the segregation of bismuth.

On the other hand, the effect of Pr-ion on the formation of interfacial states was discussed by Mukae and Nagasawa [11] from the viewpoint of the valence state of Pr-ion. They reported that a crystalline form of praseodymium oxide at the grain boundaries was Pr_2O_3 for samples annealed at high temperature and Pr_6O_{11} for the samples at low temperature. Very recently, Chun et al. [12] indicated that the phase diagram in ZnO-Pr_2O_3. In that report, existence of not Pr_6O_{11}, stable phase at room temperature, but Pr_2O_3, reduced and high temperature phase, was found in the samples.

In general, there are many methods to determine the valence state of ions in solid, e.g., chemical titration, AES, XPS, magnetic measurement etc. The merit to use the magnetic measurement is that this technique is sensitive to a valence state of magnetic ion but not sensitive to a surface state. The relation between a magnetic moment and a valence state of Pr-ion in PrO_x have been studied [13, 14]: the effective moment of Pr-ion was 2.51 μ_B for PrO_2, 2.78 μ_B for Pr_6O_{11}, 2.82 μ_B for $PrO_{1.72}$, and 3.59 μ_B for Pr_2O_3. As for PrO_2, it was shown from neutron diffraction measurements that the occurrence of antiferromag-

[†]Corresponding author.
[‡]Present address: Research Center, Sony Co., Atsugi Technology Center, 4-14-1, Asahi, Atsugi, Kanagawa 243-0014 Japan.
[§]Present address: Advanced Ceramic Technology Co., Ltd., 1-167-1 Higashi-Oume, Oume, Tokyo 198-0042, Japan.

netic ordering appeared at below 14 K resulting from an energy splitting for $J = 5/2$ multiplet [15]. Recently, the valence state of Pr-ion in some cuprate superconductors was elucidated from magnetic measurements and discussed in relation to the suppression of superconductivity for $(Y,Pr)Ba_2Cu_3O_{7-\delta}$ [16] and $(Pr,Ce,Sr)_2CuO_{4+\delta}$ [17]. It was suggested that the magnetization of Pr-ion is sensitive to the valence state and crystal field splitting [18, 19].

In the present study, valence state was investigated for Pr-doped ZnO ceramics by measuring magnetic and electric properties, and the relation between valence state of Pr-ion and nonlinear *I-V* characteristics of Pr-doped ZnO ceramic was discussed. The samples used were annealed under various conditions. The spatial distribution of Pr-ion was determined by an AES technique.

2.   Experimental

2.1.   *Preparation of Pr-doped ZnO and PrO$_x$*

Two kinds of samples were prepared: one was the Pr-doped ZnO ceramics (P-ZnO) whose atomic ratio was $Zn:Pr = 99:1$ and the other was Pr- and Co-doped ZnO ceramics (PC-ZnO) whose atomic ratio was $Zn:Pr:Co = 97.98:0.467:1.553$. Source materials were ZnO, Pr_6O_{11} and Co_3O_4. P-ZnO was sintered at 1200°C for 6 h in O_2 gas flow (1 atm) and PC-ZnO at 1310°C for 4 h in the air. The sintered samples were further annealed at 1200°C for 6 h in the air, at 800°C for 6 h in nitrogen gas flow or at 1200°C for 6 h in argon gas flow to vary their electronic property. As a reference sample, pure ZnO ceramic was prepared by the same procedure as P-ZnO.

PrO$_x$ ceramics were synthesized from Pr_6O_{11} powder which is the most stable phase in the air. Pr_6O_{11} ($x = 1.83$) was sintered at 1050°C for 12 h in the air. Pr_2O_3 ($x = 1.5$) was obtained by reducing Pr_6O_{11} at 800°C for 36 h in an evacuated tube of SiO_2 glass together with oxygen getter (sponge titanium metal). On the other hand, PrO_2 ($x = 2.0$) was prepared by oxidizing Pr_6O_{11} at 800°C for 36 h in 30 atoms of oxygen gas.

2.2.   *Analysis and Measurements*

Crystalline phases of PrO$_x$ were identified by *X*-ray powder diffraction and their crystal structures were refined by Rietveld method using a RIETAN-94 program [20].

An AES technique (Microlab 320D: VG Scientific, UK) was applied to determine the spatial distribution of Pr-ion in P-ZnO. Samples were fractured in an ultra-high vacuum and measured as soon as possible to prevent surface pollution.

Current-voltage characteristics were measured at room temperature using a dc current source (type 220: Keithley, USA) and a digital multimeter (type 195: Keithley, USA). In-Ga alloy was used as electrode to form ohmic contact.

Magnetic susceptibility was measured with a SQUID magnetometer (MPMS[2]: Quantum Design, USA) under magnetic field of 0.10T between 5 and 300 K. Magnetic-field dependence of magnetization was measured at 5 K below 5.00 T to examine the existence of spontaneous magnetization and saturation of magnetization under higher field.

3.   Results

3.1.   *Crystalline Phases of PrO$_x$ Synthesized*

PrO$_x$ samples oxidized in 30 atms of O_2 gas were cubic PrO_2 with a lattice parameter $a = 0.53926$ nm. On the other hand, PrO$_x$ samples reduced in vacuum were hexagonal Pr_2O_3 with lattice parameters $a = 0.38597$ nm and $c = 0.60162$ nm. Structural parameters refined for PrO_2 and Pr_2O_3 agreed with values reported in refs. 21 and 22. No secondary phase was observed by XRD technique.

3.2.   *AES Spectra of Praseodymium*

Figure 1 indicates AES spectra for intra-grain and grain boundary of P-ZnO. Auger transitions were observed at 90–150 eV, 460–530 eV, and 800–1020 eV which were assigned to O-*KLL*, Zn-*KVV* and Pr-*NVV* transitions, respectively. As seen in Fig. 1, Pr-ions were found at the grain boundary but not at all at the intra-grain.

3.3.   *Current-voltage Characteristics*

Figure 2 indicates current-voltage characteristics for P-ZnO and PC-ZnO. Strong nonlinear *I-V* characteristics were observed for the as-sintered samples; however, the nonlinearity diminished with the

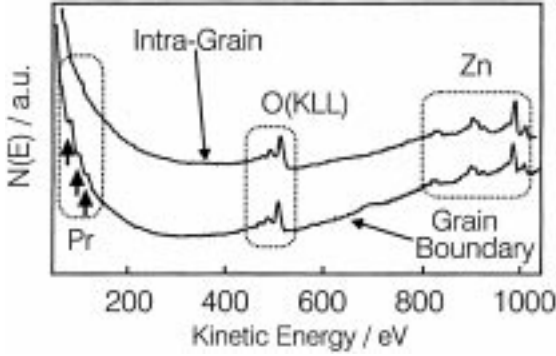Fig. 1. Typical Auger electron spectra for the grain boundary and intra-grain in ZnO ceramics doped with praseodymium oxide.

Table 1. Nonlinear current-voltage characteristics of Pr-doped ZnO (Zn : Pr = 99 : 1 in atomic ratio) and (Pr,Co)-doped ZnO ceramics (Zn : Pr : Co = 97.98 : 0.467 : 1.553 in atomic ratio)

Composition	Annealing condition		Nonlinear
	Temp. /°C	Atmosphere	parameter, α
PC-ZnO (as-sint.)	1310	Air (1atm)	3.86
PC-ZnO	800	N_2 (1atm)	1.76
PC-ZnO	1200	Ar (1atm)	0.99
P-ZnO (as-sint.)	1200	O_2 (1atm)	1.64
P-ZnO	1200	Air (1atm)	1.26
P-ZnO	800	N_2 (1atm)	1.09
P-ZnO	1200	Ar (1atm)	1.00

reduction and disappeared for P-ZnO and PC-ZnO reduced at 1200°C in Ar gas.

α-value, nonlinearity parameter for I-V characteristics was defined by $\alpha = d \log |I| / d \log |V|$. The α-value was evaluated from Fig. 2 and listed in Table 1. The α-value of PC-ZnO was higher than that of P-ZnO and both of the α-values decreased with the reduction as mentioned above.
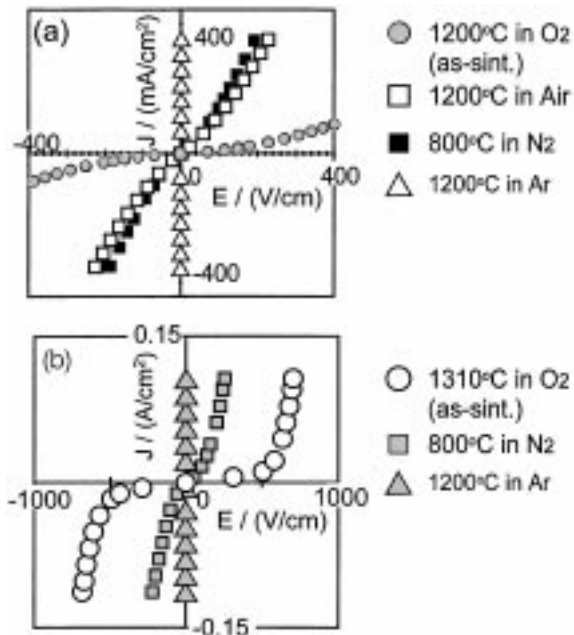

Fig. 2. Annealing effect on current-voltage characteristics for (a) Pr-doped ZnO (Zn : Pr = 99 : 1 in atomic ratio) and (b) Pr- and Co-doped ZnO (Zn : Pr : Co = 97.98 : 0.467 : 1.553).

3.4. Magnetic Susceptibility

3.4.1. PrO$_x$. Figure 3 indicates the temperature dependencies of magnetic susceptibilities χ measured for PrO_2, Pr_2O_3 and Pr_6O_{11}. The χ-T curves at higher temperature region obeyed the Curie-Weiss law:

$$\chi(T) = \frac{C}{T - \theta} + \chi_0. \qquad (1)$$

Here C is Curie constant, θ Curie-Weiss temperature and χ_0 temperature independent term of susceptibility, i.e., diamagnetism. The Curie constants and Curie-Weiss temperatures were determined from Fig. 3 by a least squares method and given in Table 2. The χ-T curves calculated from such parameters are also indicated in Fig. 3. The χ-T curves deviated from Curie-Weiss law at the lower temperature region.

The magnetization was almost proportional to the applied magnetic field at 5 K. This means that there exists no spontaneous magnetization and no saturation of magnetization occurs.

Effective number of Bohr magneton p was calculated from the Curie constant C using the following relation:

$$C = \frac{N_A p^2 \mu_B^2}{3 k_B}. \qquad (2)$$

Here, N_A is Avogadro's number, μ_B Bohr magneton and k_B Boltzman constant. The p-value observed for Pr_2O_3 was $p = 3.6$ and $p = 2.4$ for PrO_2; these values were almost in agreement with theoretical values for free Pr^{3+}-ion ($p_{cal} = 3.58$††) and Pr^{4+}-ion ($p_{cal} = 2.54$††). The p-value for PrO_x is illustrated in Fig. 4 together with p-values reported by Kern et al [13].
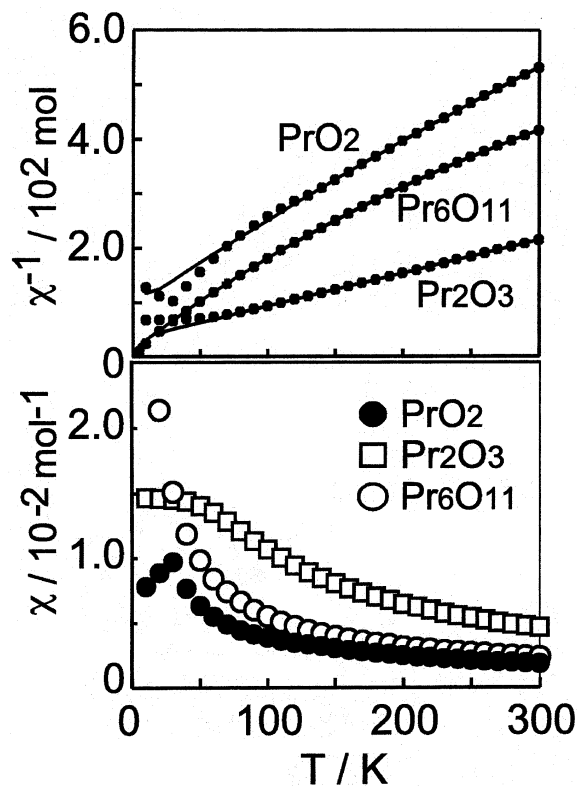
Fig. 3. Temperature dependence of magnetic susceptibility for Pr_2O_3, Pr_6O_{11} and PrO_2. Magnetic susceptibility is normalized by one mole Pr-ion. Solid lines show the best fit of $\chi(T)$ to Eq. (1) (Curie-Weiss plot) in the text.

Table 2. Curie constant C, Curie-Weiss temperature θ, temperature-independent susceptibility χ_0 and effective number of Bohr magneton p for PrO_x and Pr-doped ZnO (Zn : Pr = 99 : 1 in atomic ratio) obtained from χ-T curves shown in Figs. 3 and 5. C, θ and p were normalized by one mole of Pr-ion. Temperature range for the fitting are also listed

Sample			Curie Weiss fitting		
	C / molK	θ /K	$\chi_0/10^{-3}$ mol	p	Temperature range for fitting /K
Pr_2O_3	1.6	-63	-0.0	3.6	150–300
	1.7	-65	-0.0	3.6	70–300
Pr_6O_{11}	0.88	-75	-0.0	2.6	130–300
PrO_2	0.72	-99	-0.0	2.4	150–300
	0.71	-92	-0.0	2.4	70–300
P-ZnO	1.5	-56	-2.2	3.4	130–300
(1200°C, Ar)	1.6	-62	-2.3	3.5	70–300
P-ZnO	0.97	-25	-2.2	2.8	130–300
(800°C, N_2)	0.96	-24	-2.2	2.8	60–300
P-ZnO	1.0	-34	-1.9	2.8	130–300
(1200°C, Air)	0.96	-25	-1.8	2.8	70–300
P-ZnO	0.95	-30	-1.9	2.8	130–300
(1200°C, O_2)	0.85	-19	-1.7	2.6	70–300

3.4.2. Pr-doped ZnO. Figure 5 shows the temperature dependence of magnetic susceptibility for P-ZnO. The magnetic susceptibility obeyed the Curie-Weiss law. Curie constants C and effective number of Bohr magnetons p for Pr-ion were calculated from the χ-T curves and listed in Table 2. The p-value in P-ZnO sintered in air was $p = 2.8$ which was slightly larger than that observed for Pr_6O_{11} ($Pr^{3.78+}$), $p = 2.6$. As for the samples annealed in Ar gas, the p-value almost agreed with that of Pr_2O_3 and its χ-T curve deviated considerably from the calculated χ-T curve below 40 K; such deviation behavior was in agreement with that observed for Pr_2O_3 indicated in Fig. 3.

3.4.3. Pr- and Co-doped ZnO. Magnetic susceptibilities for PC-ZnO are given as a function of temperature in Fig. 6. Magnetization per one mole of Pr-ion was much higher for PC-ZnO than for P-

ZnO. The magnetic susceptibility $\chi(T)$ for PC-ZnO reduced in N_2 gas at 800°C almost agreed with that for PC-ZnO sintered in air, while $\chi(T)$ for PC-ZnO reduced in Ar gas at 1200°C was less than that for PC-ZnO sintered in air.

The magnetic susceptibility of pure ZnO ceramics was negative and independent of temperature in the region of 5–300 K. There was no paramagnetism in the pure ZnO ceramics even if it was annealed under reducing atmosphere.

4. Discussion

4.1. Magnetic Susceptibility of PrO_x System

The effect of crystal field spitting(CFS) of Pr$4f$ states cannot be negligible as discussed in [13] and [14]. In fact, the observed magnetic susceptibility in the lower temperature region ($T < 100$ K) was different from the Callculated value as shown in Fig. 3. This difference is due to the temperature dependence of the p-value as predicted by a CFS model [13,14]. It is thus necessary to discuss the effect of CFS in order to analyze the magnetization of Pr-ion at lower temperature. However, the p-value observed at higher temperature
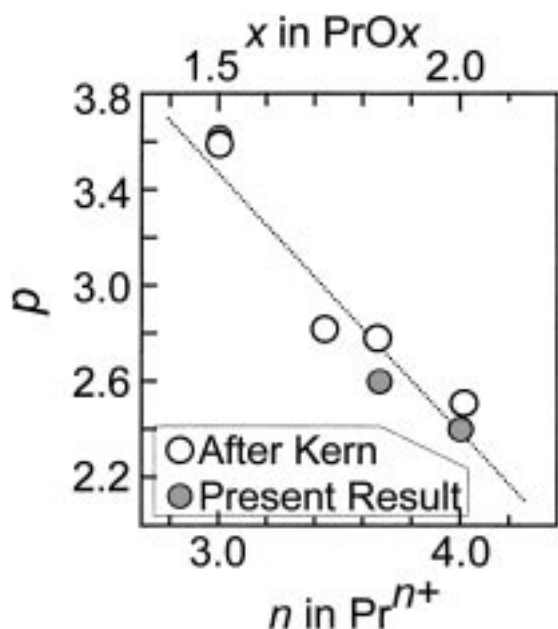
Fig. 4. Relation between x in and number of effective Bohr magneton p in PrO_x. The p-value was estimated from magnetic susceptibility at a limited temperature region listed in Table 2. Open circles are cited from S. Kern, *J. Chem., Phys.*, **40** (1964) 208.

Fig. 5. Temperature dependence of magnetic susceptibility for Pr-doped ZnO (Zn : Pr = 99 : 1 in atomic ratio) annealed under various conditions. Magnetic susceptibility was normalized for Pr-ion to be one mole.
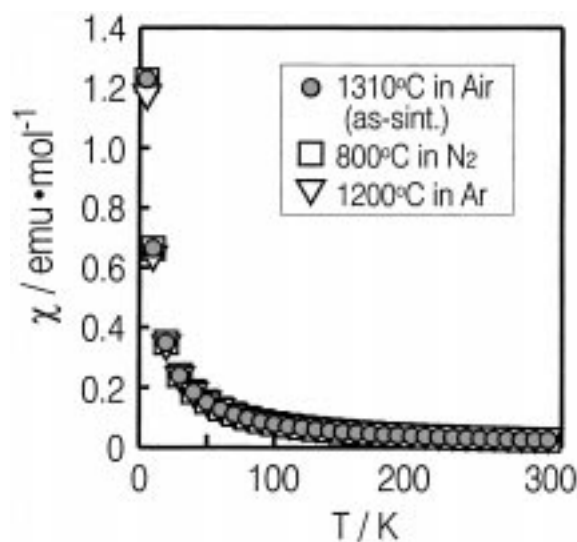
Fig. 6. Temperature dependence of magnetic susceptibility for Pr- and Co-doped ZnO ceramic (Zn : Pr : Co = 97.98 : 0.467 : 1.553 in atomic ratio) annealed under various conditions, see the text. Magnetic susceptibility is normalized by fraction of Pr-ion.

be practically evaluated from the p-value obtained from the Curie constant at higher temperature ($T > 100\,\mathrm{K}$). Assuming that the Pr-ions in P-ZnO and PC-ZnO are forming crystalline PrO_x mono-phase or mixture of PrO_x, the relation between the valence charge of PrO_x and the p-value (Fig. 4) is applicable to estimate the valence charge of Pr-ion in P-ZnO and PC-ZnO. In the discussion below, quantitative analysis of CFS model was neglected and the valence state of Pr-ion was discussed by using the p-value as a practical measure of the valence state of Pr-ion in ZnO ceramics. The effect of CFS on the χ-T curve was taken into account by comparing the χ-T curve in the lower temperature region.

4.2. Segregation and Charge of Pr-ion

From the AES measurements for P-ZnO (Fig. 1), it is indicated that the Pr-ions preferentially segregate at grain boundaries and/or triple junctions but not at grain interiors. According to secondary-electron-microscopic observations [11], the PrO_x-phase was dominantly detected at the triple junctions. Thus, it is considered that Pr-ions in P-ZnO and PC-ZnO segregate at grain boundaries and/or triple lines to form PrO_x-phases.

The p-value for P-ZnO reduced in Ar gas, abbreviated by P-ZnO/Ar, is in agreement with that

($T > 100\,\mathrm{K}$) seemed to be a function of the formal charge of Pr-ion (Fig. 4). It is consequently suggested that the valence state of Pr-ion in crystalline PrO_x can

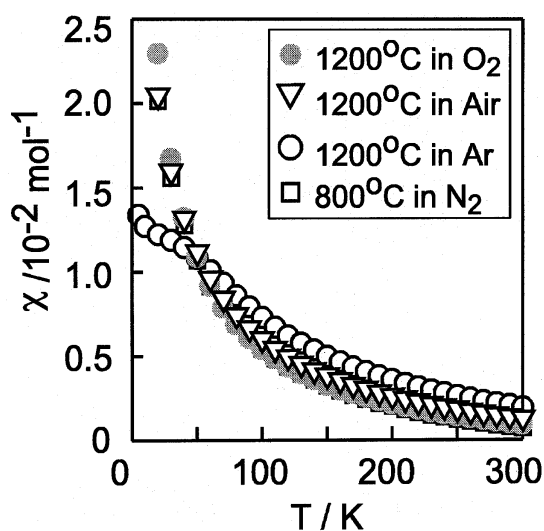for Pr_2O_3. This suggests that the Pr-ions in P-ZnO/Ar have similar valence to Pr_2O_3 in the temperature region of $T > 100$ K. Figure 7(b) shows temperature dependence of magnetic susceptibility normalized by that at 5 K to compare the temperature dependence of whole temperature region. Temperature dependence of magnetic susceptibility of P-ZnO/Ar almost agrees with that for Pr_2O_3 in whole temperature range. It is consequently suggested that the valence state of Pr-ions in P-ZnO/Ar was almost same as that in crystalline Pr_2O_3. This result is in accordance with X-ray diffraction study for intergranular materials in Pr and Co doped ZnO ceramic [11].

As for the P-ZnO samples, except for P-ZnO/Ar, the *p*-values ($p = 2.8$) evaluated in the temperature region of $T > 100$ K were adjacent to the *p*-value for Pr_6O_{11} ($p = 2.6$). The Pr-ions in P-ZnO having $p = 2.8$ is thus considered to take a mixed valence state between Pr^{3+} and Pr^{4+} or mixture of PrO_x with different *x*, since the temperature dependence of normalized magnetic susceptibility of P-ZnO shown in Fig. 7(a) seemed be different from that of Pr_6O_{11} and Pr_2O_3. It is clearly indicated that valence state of

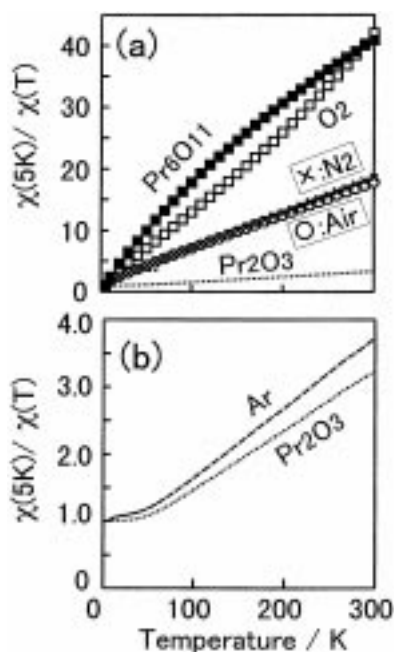*Fig. 7.* Temperature dependence of magnetic susceptibility normalized by that at 5 K for each sample. 'Pr_2O_3' and 'Pr_6O_{11}' are for pure PrO_x prepared in the present study and 'O$_2$', 'Air'. 'N$_2$' and 'Air' are for Pr-doped ZnO (Zn : Pr = 99 : 1 in atomic ratio) annealed in various atmosphere. Detail of the annealing procedure is written in the text.

Pr-ion in P-ZnO varies by the thermal treatment, even though the *p*-value of P-ZnO except for P-ZnO/Ar was almost same ($p = 2.8$). The variation of $\chi(T)$ curvature is considered to be due to change in effective charge and coordination structure of Pr-ion in ZnO ceramics. As indicated in [21] and [22], both charge and crystalline form of PrO_x are changed with oxygen partial pressure. Thus, variation of $\chi(T)$ curvature indicated in Figs. 7 suggests that chemical state of PrO_x in grain boundary region of P-ZnO is modified by thermal treatment.

As mentioned before, the pure PrO_x sample has the Pr_6O_{11} phase when sintered in the air and O_2 atmosphere. On the contrast, the P-ZnO samples took the different valence state from Pr_6O_{11} though they were sintered in the same atmosphere, as indicated in Fig. 7. This behavior indicates that the Pr-ions tend to be easily reduced in P-ZnO than in pure PrO_x. The reduction of dopant in grain boundary region was also observed for the Bi-doped ZnO ceramics[7,8] in which the oxygen content at grain boundaries with Bi was less than that at both grain boundary without Bi and at the intra-grain. The present result on the valence state of Pr-ions is consistent to that of Mukae and Nagasawa [11] indicating that the Pr-ion is reduced to form Pr_2O_3 at brain boundary in in ZnO ceramics. However, $\chi(T)$ curvature of P-ZnO sintered in air or nitrogen gas disagreed with that of Pr_2O_3, even though the intergranular material in Pr and Co doped ZnO ceramic was identified to be Pr_2O_3 by X-ray diffraction study reported in [11]. The origin of the difference in present result and [11] is considered to be due to the difference in sensitivity of the method to detect the chemical state or difference in kind and/or amount of dopant. The magnetization of Co doped ZnO will be discussed in the next section.

(3) *I-V Characteristics and Charge of Pr-ion*

Figure 8 shows the relation between the α-value and the effective number of Bohr magnetons *p* for Pr-ion in the P-ZnO ceramics. As shown in Fig. 8, the α-value steeply decreased with the increase of the *p*-value and the nonlinear *I-V* characteristics disappeared (i.e., α = 1.0) when the Pr-ion was reduced, i.e, $p \geq 2.8$.

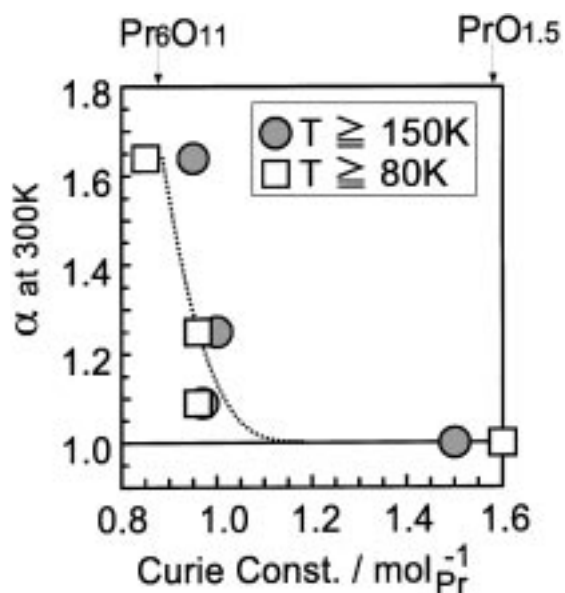The Pr-ions segregate at the triple lines as described above. It is considered that the triple lines

Fig. 8. Nonlinear parameter α versus effective number of Bohr magneton p for Pr-ion observed for Pr-doped ZnO samples (Zn : Pr $= 99 : 1$ in atomic ratio). Definition of α and p are described in the text. The value of p are calculated for temperature range of $80 \leqq T \leqq 300$ and $150 \leqq T \leqq 300$.

have no direct influence to the *I-V* characteristics, since the electric current does not pass the triple lines. Thus, the nonlinear *I-V* characteristics should not be directly dependent of the valence state of the Pr-ions in the triple junctions. Nevertheless, the *I-V* characteristics change with the valence state of the Pr-ions as shown in Fig. 8. It is consequently considered that the valence state of the Pr-ions at the grain boundaries changes corresponding to that of the triple lines as the grain boundaries are in a chemical equilibrium with the triple lines.

In the PC-ZnO system, it is difficult to find the relation between the α- and p-values, since both Pr-ion and Co-ion have the magnetic moments which are impossible to be separated from the χ-T curve. However, as the magnetic moment of PC-ZnO is very large in comparison with that of P-ZnO, the magnetic moment is mainly ascribed to the Co-ions. Therefore, the p-value of the Co-ion in PC-ZnO was estimated to be $p = 4.4$. The p-value for the Co^{2+} ion is expected to be $p_{cal} = 6.63$ supposing orbital angular momentum is not quenched[‡‡] and $p_{cal} = 3.87$ supposing the orbital angular momentum is quenched[§§]. The valence state of the Co-ion in PC-

ZnO is consequently adjacent to Co^{2+} in which the orbital angular momentum is partially quenched.

The magnetic susceptibility for PC-ZnO decreased after the reduction in Ar gas at 1200°C; the change is very small as seen in Fig. 6 but can be apparently observed. The magnetic susceptibility change due to the reduction is thus ascribed to the change in the valence state of the Pr-ions and the valence state of the Co-ion is plausibly unchanged. Corresponding to this change, the α-value simultaneously decreased from 3.9 to 1.0. Therefore, the valence state of the Pr-ion is also modified in the PC-ZnO system by the reduction process, and the nonlinear *I-V* characteristics is suppressed with the reduction of the Pr-ion as is similar to the P-ZnO system.

The α-value is enhanced from $\alpha = 1.64$ (P-ZnO) to $\alpha = 3.86$ (PC-ZnO) by the addition of Co-ion; however, in spite of the existence of Co-ions, the reduction of the α-value for the PC-ZnO is very similar to that for P-ZnO. This means that the valence state of Pr-ions is essential to form the interfacial states while the Co-ions might change the barrier height probably through controlling a donor concentration in the grain.

5. Summary

Magnetic properties of Pr-doped ZnO were studied in relation to nonlinear *I-V* characteristics. The Pr-ion in the ZnO ceramics sintered in the air had an electric charge between Pr_2O_3 and Pr_6O_{11}. The Pr-ion segregated at triple lines and grain boundaries in the ZnO ceramics, and their valence state was more reduced than pure Pr_6O_{11} even though they were sintered in the same oxidizing condition. Effective number of Bohr magnetons were changed by reduction in Ar/N$_2$ gases and the nonlinearity of *I-V* characteristics varied corresponding to the change in the valence state of Pr-ions. Nonlinear *I-V* characteristics disappeared when the Pr-ion was reduced near to Pr^{3+} state.

Notes

†† pl: $p_{cal} = g\sqrt{J(J+1)}$ $g = 0.800, J = 4$ for Pr^{3+} and $g = 0.857$, $J = 5/2$ for Pr^{4+}.
‡‡ $p_{cal} = g\sqrt{J(J+1)}$: $g = 1.333, J = 4.5$.
§§ $p_{cal} = 2\sqrt{S(S+1)}$: $S = 2.5$.

References

1. M. Matsuoka, *Jpn. J. Appl. Phys.*, **10**, 736 (1971).
2. K. Mukae, K. Tsuda, and I. Nagasawa, *Jpn. J. Appl. Phys.*, **16**, 1361 (1977).
3. L. M. Levinson and H. R. Philipp, *J. Appl. Phys.*, **46**, 1332 (1975).
4. G. Blatter and F. Greuter, *Phys Rev. B*, **33**, 3952 (1986).
5. T. Maeda and M. Takata, *Yogyo Kyokaishi*, **97**, 1221 (1989).
6. H. Okushi and Y. Tokumaru, *Jpn. J. Appl. Phys.*, **19**, L335 (1980).
7. J. Tanaka, H. Haneda, S. Hishita, F. P. Okamura, and S. Shirasaki, *Materials Science Forum Colloque de Physique C1, Supplément*, **51**, C1–1055 (1990).
8. S. Tanaka, C. Akita, N. Ohashi, J. Kawai, H] . Haneda, and J. Tanaka, *J. Solid State Chem*, **105**, 36 (1993).
9. N. Ohashi, S. Tanaka, C. Akita, J. Kawai, H. Adachi, O. Fukunaga, and J. Tanaka, in *Computer Aided Innovation of New Materials II* (Elsevier Science, Amsterdam, 1993) p. 1557.
10. N. Ohashi, S. Tanaka, T. Tsurumi, J. Tanaka, and O. Fukunaga, *J. Ceram. Soc. Jpn.,* **106**, 914 (1998).
11. K. Mukae and I. Nagasawa, *Advance in Ceramics Vol. 7 Additives and Interfaces in Electronic Ceramics*, edited by M. F. Yan and H. Heuter (Am. Ceram. Soc. Inc., OH, USA).
12. S.-Y. Chun, N. Wakiya, H. Funakubo, K. Shinozaki, and N. Mizutani, *J. Am. Ceram. Soc.*, **80**, 995 (1997).
13. S. Kern, *J. Chem., Phys.*, **40**, 208 (1964).
14. J. B. MacChesney, H.J. Williams, R. C. Sherwood, and J. F. Potter, *J. Chem., Phys.*, **41**, 3177 (1964).
15. S. Kern, C.-K. Loong, J. Faber Jr., and G. H. Lander, *Solid State Comm.*, **49**, 295 (1984).
16. B. Fisher, J. Genossar, L. Patlagan, and J. Ashkenazi, *Phys. Rev. B*, **43**, 2821 (1991).
17. N. Ohashi H. Ikawa, O. Fukunaga, M. Kobayashi, and J. Tanaka, *Physica C*, **177**, 377 (1991).
18. L. Soderholm, C. K. Loong G. L. Goodman, and B. D. Dabrowski, *Phys. Rev. B*, **43**, 7923 (1991).
19. R. S. Puche, M. Norton, T. R. White, and W. S. Glaunsinger, *J. Solid State Chem.*, **50**, 281 (1983).
20. Y. Kim and F. Izumi, *J. Ceram. Soc. Jpn.*, **104**, (1994) 401.
21. E. D. Guth, J. R. Holden, N. C. Baenzinger, and L. Eyring, **76**, 5239 (1954).
22. C. L. Sieglaff and L. Eyring, *J. Amer. Ceram. Soc.*, **79**, 3024 (1957).